Molecular Determinants of Xenobiotic Metabolism: QM/MM Simulation of the Conversion of 1-Chloro-2,4-dinitrobenzene Catalyzed by M1-1 Glutathione S-Transferase†

Anna L. Bowman,‡ Lars Ridder,§ Ivonne M. C. M. Rietjens,|| Jacques Vervoort,⊥ and Adrian J. Mulholland*,‡

Centre for Computational Chemistry, School of Chemistry, University of Bristol, Cantock's Close, Bristol BS8 1TS, U.K., Molecular Design and Informatics, N. V. Organon, The Netherlands, Division of Toxicology, Wageningen University, Tuinlaan 5, 6703 HE Wageningen, The Netherlands, and Laboratory of Biochemistry, Wageningen University, Dreijenlaan 3, 6703 HA Wageningen, The Netherlands

Received November 3, 2006; Revised Manuscript Received February 12, 2007

ABSTRACT: Modeling methods allow the identification and analysis of determinants of reactivity and specificity in enzymes. The reaction between glutathione and 1-chloro-2,4-dinitrobenzene (CDNB) is widely used as a standard activity assay for glutathione S-transferases (GSTs). It is important to understand the causes of differences between catalytic GST isoenzymes and the effects of mutations and genetic polymorphisms. Quantum mechanical/molecular mechanical (QM/MM) molecular dynamics simulations have been performed here to investigate the addition of the glutathione anion to CDNB in the wild-type M1-1 GST isoenzyme from rat and in three single point mutant (Tyr6Phe, Tyr115Phe, and Met108Ala) M1-1 GST enzymes. We have developed a specifically parameterized QM/MM method (AM1-SRP/CHARMM22) to model this reaction by fitting to experimental heats of formation and ionization potentials. Free energy profiles were obtained from molecular dynamics simulations of the reaction using umbrella sampling and weighted histogram analysis techniques. The reaction in solution has also been simulated and is compared to the enzymatic reaction. The free energies are in excellent agreement with experimental results. Overall the results of the present study show that QM/MM reaction pathway analysis provides detailed insight into the chemistry of GST and can be used to obtain mechanistic insight into the effects of specific mutations on this catalytic process.

Glutathione S-transferases (GSTs[1]) are a widely distributed family of detoxification enzymes, which catalyze the conjugation of the tripeptide glutathione (γ-Glu-Cys-Gly) to a wide range of compounds. This reaction is an important step in the detoxification of a large variety of xenobiotic compounds including many carcinogens and toxins in mammals and other organisms (*1*). GSTs are an example of phase II metabolizing enzymes, which conjugate an endogenous hydrophilic molecule to reactive electrophilic xenobiotics thereby detoxifying them and/or facilitating their excretion from the organism. At least 19 different glutathione S-transferase isoenzymes have been found in the human genome (http://www.ncbi.nlm.nih.gov/genome/guide/human/). This is a remarkably high number given that the human genome codes for only 20,000−25,000 unique genes (*2*). The differential expression of these enzymes has been implicated in resistance to chemotherapeutic drugs (*3*). GSTs exhibit a wide range of substrate specificities, which is achieved not only by distinct classes of GST enzymes but also by the fact that an isoenzyme can be specifically catalytically active toward a large variety of exogenous substrates. GSTs also show distinct genetic polymorphisms which can alter the enzyme's activity (*4*). A fuller understanding of the catalytic mechanism of GSTs and the effects of mutations is therefore intrinsically important, for example to understand and eventually predict the biological consequences of SNPs (single nucleotide polymorphisms).

The reaction between glutathione (GSH) and 1-chloro-2,4-dinitrobenzene (CDNB) is catalyzed by different GST isoenzymes (*4*), and is widely used as a standard activity assay for glutathione S-transferases (*5*) (Figure 1). Hence, studying this catalytic reaction in particular may help to understand the differences between GST isoenzymes and the effect of genetic polymorphisms. There is a need for computational simulation techniques capable of dealing accurately with this challenging reaction. The abundance of experimental data relating to this system provides a stringent test and validation of modeling techniques.

The five genes encoding the Mu class of GST enzymes are organized in a gene cluster on chromosome 1p13.3, have high sequence identity (80−90%), and are known to be

† This research has been supported by the EPSRC, BBSRC, IBM Life Sciences Outreach Programme and a Marie Curie Fellowship of the European Community program Quality of Life within the fifth framework under Contract QLRI-CT-1999-51244.

* Author to whom correspondence should be addressed. Tel: +44 (0)117 928 9097. Fax: +44 (0)177 925 1295. E-mail: Adrian.Mulholland@bristol.ac.uk.

‡ University of Bristol.

§ N. V. Organon.

|| Division of Toxicology, Wageningen University.

⊥ Laboratory of Biochemistry, Wageningen University.

[1] Abbreviations: CDNB, 1-chloro-2,4-dinitrobenzene; GST, glutathione S-transferase; QM/MM, quantum mechanical/molecular mechanical; AM1-SRP, specifically parameterized version of AM1 (specific reaction parameters); GSH, glutathione; SD, steepest descent.

10.1021/bi0622827 CCC: $37.00
Published on Web 05/05/2007

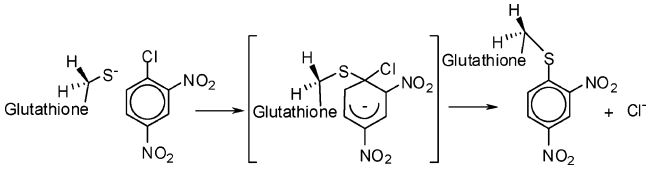

FIGURE 1: The conjugation of glutathione anion with CDNB via the Meisenheimer complex (center).

highly polymorphic (http://www.ncbi.nlm.nih.gov/entrez/query.fcgi?db=gene&cmd=Retrieve&dopt=Graphics&list_uids=2944). Different Mu class glutathione S-transferases show major differences in the substrate specificity. A library of variant GST M1-1 and GST M2-2 enzymes has been created and tested for its catalytic activity toward a set of substrates, including CDNB, by the group of Mannervik (*6*). The rates of reaction were shown to vary up to 5 orders of magnitude. Recently, amino acid residues of the Mu class GSTs which give rise to the functional catalytic diversity in this class of enzymes have been studied (*7*). It has been shown by Ivarsson and co-workers that the catalytic efficiency toward a set of substrates can differ strongly in the Mu class of GSTs (*7*). An accurate and well-calibrated approach for understanding the catalytic reaction mechanism of the Mu class of GSTs is therefore of great importance.

Experimental work (*8*−*11*) points to three mutations (Tyr6Phe, Tyr115Phe, and Met108Ala) which may affect the catalytic activity of Mu class GSTs. Spectroscopic and kinetic experiments show that Tyr6 is a vital residue for catalysis (*8*). The hydroxyl group of Tyr6 is part of the electrostatic environment of the active site that lowers the pK_a of the GSH thiol bound to GST. The pK_a for GSH in solution is 9.0; it drops to 6.2 when bound to the wild-type enzyme; and it is somewhat higher at 7.8 when bound to the Tyr6Phe mutant (*11*).

Affinity labeling (*12*) and crystallographic data (*13*) show that Tyr115 is located in or near the active site of Mu class GSTs, and kinetic evidence (*9*) indicates that this residue is involved in both the chemical and physical steps of the reaction mechanism. Tyr115 has also been found to be important in simulations of GST converting phenanthrene 9,10-oxide (*14*). Experimental work has shown that replacement of Tyr115 with phenylalanine (Tyr115Phe) results in a 100-fold decrease in catalytic activity with this substrate (*15*). However, with the CDNB substrate the same mutation results in a slightly more effective catalyst (an increase in k_{cat} from 20 s^{-1} to 72 s^{-1}) (*9*). It is thought that the rate-limiting step in the turnover of CDNB with GST M1-1 is product release, as shown by stopped-flow fluorescence measurements and viscosity effects on the steady-state kinetics (*9*, *16*). The Tyr115Phe mutation brings about the loss of hydrogen bonds between the hydroxyl group of Tyr115 and the side chain hydroxyl group and main chain NH of Ser209. These hydrogen bonds are thought to block the channel to the active site or inhibit the segmental motion of the protein (*9*).

Met108 has been thought to play a key role in the binding of CDNB. The steady-state kinetic parameters of the wild-type human M2-2 GST with CDNB and GSH have been studied experimentally, and compared to the Met108Ala mutant enzyme (*10*). Substitution of Met108 with Ala leads to no change in the steady-state mechanism or in the binding of GSH. However, there is a decrease in V_{max}/K_{mCDNB}, from which it was deduced that the Met108Ala mutant leads to a reduction in affinity for CDNB (*10*). The mutation has also been reported to result in a slight increase in the turnover (by a factor of 1.7), indicating that the mutation has a small effect on the rate-limiting step in catalysis (*10*).

In the present study, a specifically parameterized combined quantum mechanical/molecular mechanical (QM/MM) method has been developed and applied to model the reaction of glutathione with CDNB in the M1-1 GST isoenzyme from rat. QSAR studies on the GST catalyzed conversion of nitrobenzenes have shown that electronic parameters are of great importance in catalysis (*17*, *18*). Free energy profiles have been calculated for the two step S_NAr addition/elimination mechanism. The reaction is also simulated in three single point mutant enzymes (Tyr6Phe, Met108Ala, and Tyr115Phe) for comparison with experiments. The QM/MM umbrella sampling molecular dynamics approach allows for flexibility of the enzyme active site, CDNB and glutathione, and for explicit solvation of the enzyme. The QM/MM approach, introduced for enzyme reactions by Warshel and Levitt (*19*), treats the central reacting system by a quantum chemical method, while representing the remainder of the system by a classical empirical force field model. The QM/MM method can provide insight into an enzyme's mechanism beyond that achievable by experimental methods, e.g., by the direct visualization and analysis of the transition state and unstable intermediates (*20*). Here we have developed and applied a reaction specific QM/MM method (AM1-SRP/CHARMM22), which we have specifically parameterized for the GSH/CDNB reaction, to obtain reliable energetics and efficient conformational sampling. Specific parameterization of semiempirical molecular orbital methods is a good way to overcome their known limitations (*14*, *21*, *22*). Reaction specific parameterization of the QM/MM approach is analogous to the empirical valence bond (EVB) method, in which the reacting system is represented by a combination of simple empirical resonance forms (*23*). When the incorporated empirical terms are carefully chosen, the EVB approach can produce highly accurate results (*24*). Here, though, we apply molecular orbital electronic structure quantum chemical techniques.

Reactions of the S_NAr type usually proceed via a σ-complex, often called the Meisenheimer complex (Figure 1). It is not clear whether the Meisenheimer complex is a true intermediate or a transition state. Unstable and short-lived intermediates in condensed phase reactions are generally very difficult to isolate or study directly by experiment. Computational techniques have the potential to model transition states and reaction intermediates, and to identify and analyze interactions responsible for stabilizing these species in enzymes. The stability of Meisenheimer complexes in GST enzymes has not previously been investigated to our knowledge. The reaction between glutathione and 1-chloro-2,4-dinitrobenzene in the gas phase and in solution (using a dielectric continuum solvent model) has been investigated by Zheng and Ornstein (*25*). These *ab initio* studies found the Meisenheimer complex to be a true intermediate in solution with a 1.6 kcal mol^{-1} barrier to loss of the chloride. Recently, QM/MM free energy simulations of the conversion of 4-chlorobenzoate to 4-hydroxybenzoate catalyzed by 4-chlorobenzoyl-CoA dehalogenase showed significant sta-

bilization of the Meisenheimer complex by the enzyme, resulting in a discrete intermediate along the reaction path of this S_NAr mechanism (*26*). In studies of GSH with 1,3,5-trinitrobenzene, which may be a inhibitor of the enzyme, a relatively stable Meisenheimer complex is observed (*27*) experimentally, but a similar complex has yet to be detected for CDNB. The objective of the present study is to characterize reaction of glutathione with CDNB catalyzed by the M1-1 GST isoenzyme, in three mutant enzymes, and also the uncatalyzed reaction in solution, and to compare the results with experimental findings. To obtain reliable results, we have optimized system specific AM1-SRP parameters, and applied these in QM/MM molecular dynamics simulations of the reaction. The use of a specifically parameterized and validated QM/MM model should provide reliable energetics for this challenging reaction. We have previously demonstrated the success of this approach in a study of the reaction of glutathione with phenanthrene 9,10-oxide catalyzed by M1-1 GST (*14*). Here, we have examined the effects of the protein, in comparison to the uncatalyzed reaction of glutathione with CDNB in solution, and we have investigated the stability of the Meisenheimer complex. We discuss the results and their implications for understanding GST mediated catalysis and the consequences for reaction of some mutations.

METHODS

Simulation System. The starting models for the simulations were based on the crystal structure of rat liver M1-1 glutathione S-transferase in complex with a transition state analogue 1-(*S*-glutathionyl)- 2,4,6-trinitrocyclohexadientate (*28*). This structure was altered to give the Meisenheimer complex 1-chloro-1-(*S*-glutathionyl)-2,4-dinitrocyclohexadienate as shown in Figure 1. The methods employed here have previously been used successfully to model GSTs and other enzymes (*14*, *29*−*31*). The procedure for the model setup was similar to that used in simulations of the conjugation of glutathione to phenanthrene 9,10-oxide in M1-1 GST (*14*). Hydrogen atoms were placed using the HBUILD routine in CHARMM. The high computational demands of QM/MM dynamics calculations necessitates that a balance must be struck between system size and the extent of sampling. The experimentally determined structures of the enzyme bound transition state analogue (PDB ID: 4GST the starting structure here), the product complex (PDB ID: 5GST), and the unliganded enzyme (PDB ID: 6GST) are very similar. Comparison of these structures shows that there is essentially no change in conformation associated with reaction. It is therefore appropriate for the simulations to focus on the active site and its immediate environment using a stochastic boundary approach (*32*). The simulation system contained an approximately spherical selection of residues centered on the C_1 atom of the substrate (atom numbering is shown in Figure 7). All protein residues and crystal waters with at least one atom within 18 Å of the center were selected. The system was then solvated by superimposing an 18 Å radius sphere of pre-equilibrated CHARMM TIP3P water molecules (*33*) and deleting any added water molecule of which the oxygen was within 2.6 Å distance of another non-hydrogen atom. Minimization of water molecules (only) with 100 steps of steepest descent (SD) was performed. Then 10 ps of Langevin dynamics (300K) for all water molecules (all other atoms fixed) was carried out, finally minimizing again with 100 steps of SD.

The QM region (i.e., 1-chloro-2,4-dinitrobenzene and the cysteine side chain of glutathione, 21 atoms in total) was treated with a system-specific version of AM1 (see below). In order to describe the bond crossing the QM/MM boundary, a link atom was placed between the Cα and C*β* of the cysteinyl side chain of glutathionyl. The link atom was a QM hydrogen without classical van der Waals or bonded force field terms. It did, however, interact with all MM charges except the host group. It has been shown that better results are obtained if the link atom interacts with the entire MM system apart from the few closest bonded classical atoms (*34*). Hence, the Cα and Hα of the cysteinyl side chain of glutathionyl were neutralized. The overall charge on the QM system was −1. All other atoms (2661 in total) were treated by molecular mechanics, using the CHARMM22 all-atom force field (*33*, *35*).

Throughout, a 2 Å buffer zone was defined as all atoms further than 16 Å away from the center of the sphere, in which the nonsolvent heavy atoms were harmonically restrained to their crystal coordinates with force constants based on model average *B*-factors (*32*, *36*). This is a larger simulation system than that used in our previous work on M1-1 GST with phenanthrene 9,10-oxide, which used a radius of 14 Å (*14*). The buffer restraints were scaled (linearly and in four steps) from zero at 16 Å away from the center of the system, to a maximum at 18 Å. In the simulations, Langevin dynamics was applied for the buffer region (updated every 50 steps), using friction coefficients of 250 ps^{-1} for non-hydrogen protein atoms, and 62 ps^{-1} for the water oxygens (*32*). A deformable boundary potential was applied to restrain the water molecules to remain within the 18 Å sphere. SHAKE was applied to fix all MM bonds involving hydrogen atoms, and a 1 fs time step was used. All simulations were carried out with the CHARMM program version 27b2 (with some local modifications) (*37*).

Umbrella Sampling Molecular Dynamics Free Energy Simulations. The Meisenheimer complex was used as the starting structure for subsequent umbrella sampling molecular dynamics simulations (*14*, *31*, *38*). The reaction coordinate was defined in terms of the breaking and forming bond distances as $r_1 = d(Cl-C_1) - d(SG2-C_1)$, a more positive value indicating a larger $Cl-C_1$ distance (e.g., products) and a more negative value corresponding to a larger $SG2-C_1$ distance (e.g., reactants). Similar reaction coordinates have previously been successfully applied (*14*). The reaction coordinate was restrained harmonically to a range of values (at every ± 0.1 Å starting at 0.0 Å) along the reaction coordinate with a force constant of 100 kcal mol^{-1} $Å^{-2}$. A separate QM/MM molecular dynamics simulation was performed at every reaction coordinate value. Each simulation consisted of 50 steps of steepest descent minimization and 10 ps of equilibration followed by 20 ps of sampling dynamics. Each subsequent simulation was started from the 10 ps point of the adjacent run. The reaction coordinate statistics of the various simulations were combined by means of the weighted histogram analysis method (*39*, *40*).

The reaction coordinate definition described above was found to result in some unwanted behavior at large negative values of the reaction coordinate, i.e., the glutathione anion attacked C5 of CDNB. Additional simulations with the

reaction coordinate, $r_2 = d(SG2-C_1)$, the $Cl-C_1$ distance restrained to a value of 1.72 Å with a force constant of 100 kcal mol^{-1} $Å^{-2}$, were performed. This value was chosen from the mean average $Cl-C_1$ distance (1.72 Å ± 0.04 Å from simulations with r_1 between −2.0 and 0.0 Å). The reaction coordinate was sequentially restrained harmonically to a range of values (at every 0.1 Å starting at $d(SG2-C_1) =$ 1.7 Å) along the reaction path. This new setup enabled reactant geometries with a larger distance (up to 3 Å) between the thiolate and CDNB ring to be sampled.

Structural Analysis. Structures along the reaction coordinate were analyzed for important interactions between the substrate, protein, and solvent. For each simulation (i.e., for every value along the reaction coordinate) 20 structures, taken from the dynamics trajectory every 0.5 ps, were analyzed (740 structures in total along the reaction pathway). A hydrogen bond was defined as a hydrogen to acceptor distance of less than 2.5 Å (2.8 Å if the donor is sulfur) and the angle between atoms forming the hydrogen bond was greater than 90° (*41*).

Reaction Specific (AM1-SRP) Parameterization. We have previously demonstrated significantly improved description of a GST-catalyzed reaction by a specifically reparameterized version of AM1 (*14*). A similar approach was applied here. The energies of the σ-adduct intermediate and the conjugation product, relative to the reactants (Figure 1), are the most important values to describe correctly. The parameters of the original AM1 method were derived based on experimental data (*42*), and similarly here we optimized AM1-SRP parameters by fitting to experimental data, such as measured heats of formation. Parameter optimization directly toward correct energies for the reaction studied here is complicated by the lack of an experimental heat of formation of the σ-complex intermediate, and by the unstable nature of this intermediate. Therefore, we chose to optimize AM1 to reproduce experimental heats of formation and ionization potentials for a number of relevant molecules in the gas phase, and to validate the results by comparing the AM1-SRP energies for the conjugation reaction (in the gas phase) to higher-level QM calculations.

Experimental heats of formation and ionization potentials were obtained from the NIST Standard Reference Database (http://webbook.nist.gov/chemistry/). Optimization of S, Cl, O, and N parameters was performed using a genetic algorithm similar to that described by Bash et al. (*43*) and implemented as a modification to the libGA code by Corcoran and Wainwright (*44*). For full details of the genetic algorithm set up see Ridder et al. (*14*). The AM1-SRP parameters are given in Supporting Information.

Table 1 presents the experimental, AM1, and AM1-SRP values of heats of formation and ionization potentials for the selected relevant molecules. To confirm that the resulting AM1-SRP model does indeed provide an improved treatment of the reaction, the energies of the reactants, intermediate, and products (as shown in Figure 1) were calculated in the gas phase (with GS^- modeled as CH_3S^-) at the HF/6-31G(d), B3LYP/6-31+G(d)//HF/6-31G(d), and MP2/6-31+G(d)//HF/6-31G(d) levels as well as AM1 and AM1-SRP. The relative energies corresponding to step 1 and step 2 at the various levels are presented in Table 2. The results indicate that our AM1-SRP model gives significantly improved energies in the gas phase for the reaction studied. The AM1-SRP energies are much closer to the MP2/6-31+G//HF/6-31G(d) results than standard AM1.

Table 1: Experimental and Calculated of Heats of Formation (kcal mol^{-1}) and Ionization Potentials (eV) for the Selected Relevant Molecules[a]

molecule	element reparameterized	param	exptl value	AM1	AM1-SRP
methylthiolate	S	ΔH_f	−14.3	−16.99	−14.29
methylthiolbenzene	S	ΔH_f	23.3	21.02	23.30
		IP	7.94	8.13	8.06
chloride	Cl	ΔH_f	−54.36	−37.66	−54.33
		IP	3.6	2.89	3.61
chlorobenzene	Cl	ΔH_f	13	14.72	13.0
		IP	9.07	9.56	9.75
		dipole	1.72	1.3	1.90
phenol	O	ΔH_f	-23	−22.32	−23.74
		IP	8.49	9.12	8.87
		dipole	1.45	1.24	0.911
phenolate	O	ΔH_f	−38.3	−41.05	−38.09
nitrophenol	O, N	ΔH_f	−27.4	−19.68	−27.39
		IP	9.1	10.07	9.59
nitrophenolate	O, N	ΔH_f	−63.9	−65.10	−63.92

[a] AM1 results were calculated using standard parameters. AM1-SRP results were calculated with specific reaction parameters, developed in this work.

Table 2: Calculated Energies (Enthalpies for AM1 and AM1-SRP) in kcal mol^{-1} for Reaction Steps 1 and 2, and for the Overall Reaction of Methyl Thiolate with CDNB in the Gas Phase (See Figure 1)

level	step 1	step 2	overall ΔE	overall ΔH^a
HF/6-31G(d)	−31.20	−7.03	−38.23	−35.27
B3LYP/6-31+G(d)//6-31G(d)	−41.35	2.24	−39.11	−36.15
MP2/6-31+G(d) //6-31G(d)	−47.93	9.30	−38.63	−35.67
AM1	−54.96	37.83	−17.13	−17.13
AM1-SRP	−46.95	15.06	−31.89	−31.89

[a] Includes unscaled thermal corrections to the *ab initio* calculations calculated at the HF/6-31G(d) ab initio level.

Modeling of Mutations. The results of site-directed mutagenesis experiments can be interpreted by performing free energy calculations with the mutation modeled in the MM region of a QM/MM system (for residues that do not participate in covalent bonding changes in the reaction) (*14*, *45*). The three mutations modeled here (Tyr6Phe, Tyr115Phe, and Met108Ala) do not involve an increase in the number of atoms, and any structural changes are expected to be small. In the case of the Tyr115Phe mutation, for example, the hydroxyl group was deleted and an additional hydrogen was added, and the charges were changed to the standard values of those of a phenylalanine residue in the CHARMM22 MM force field (*33*). Following mutation, umbrella sampling molecular dynamics simulations were performed as described earlier for the wild-type system. Each simulation consisted of 50 steps of steepest descent minimization and 10 ps of equilibration followed by 20 ps of sampling dynamics.

RESULTS AND DISCUSSION

Simulation of Reaction in Wild-Type GST. A free energy profile for the GST reaction in the wild-type enzyme was calculated based on the reaction coordinate $r_1 = d(Cl-C1) - d(SG2-C1)$ (Figure 2). The profiles are aligned relative to the Meisenheimer complex as the zero of free energy. The absolute free energies between reactions cannot be

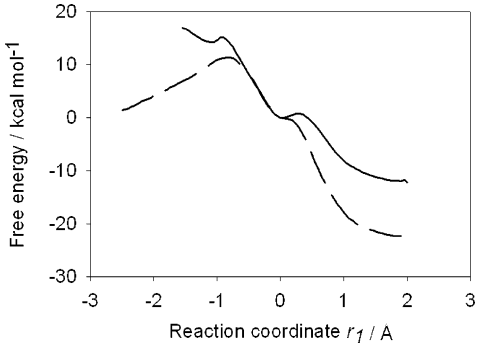

FIGURE 2: Free energy profiles for the reaction of glutathione anion with CDNB in wild-type M1-1 glutathione transferase (solid line); and for the nonenzymic reaction (addition of glutathione anion to CDNB and the elimination of chloride) in solution (dashed line). The curves are aligned taking the Meisenheimer complex as the zero of free energy in each case.

compared directly; meaningful comparisons can only be made between barriers and reaction energies.

In the enzyme, there is a small barrier (at a reaction coordinate value of $r_1 = -0.9$ Å) to forming the Meisenheimer complex from the glutathione anion and CDNB of ~1 kcal mol^{-1} (Figure 2). The energy change for complex formation is ~−13.7 kcal mol^{-1}. Formation of the Meisenheimer complex in the enzyme is calculated to be highly favorable. A shallow minimum, corresponding to the Meisenheimer complex, is present at $r_1 = 0.0$ Å. There is approximately a 1 kcal mol^{-1} barrier for dissociation of chloride from this intermediate. In a (AM1-SRP/CHARMM22) optimized structure of this intermediate, the C_1-C_2 and C_6-C_1 bond distances are 0.07 Å longer than in CDNB. The C_1-Cl and C_1-S bond distances are similar to each other (1.86 Å and 1.82 Å, respectively). The increase in C_1-C_2 and C_6-C_1 bond lengths and the similarity of the C_1-Cl and C_1-S bond distances indicate that this structure is a Meisenheimer complex (Figure 1). The calculated free energy change for chloride dissociation from the Meisenheimer complex is ~−13.9 kcal mol^{-1}. This shows that the Meisenheimer complex is a very unstable intermediate in the enzyme. Dissociation of chloride is highly favorable, and will be further favored by its full release into aqueous solution.

Another reaction coordinate (r_2) was also tested for simulating the reaction, which allowed sampling of larger distances (up to 3 Å) between the thiolate and CDNB ring. The simulations with the r_2 reaction coordinate ($r_2 = d(SG2-C_1)$) and the $Cl-C_1$ distance restrained showed the barrier to form the Meisenheimer complex to be similarly small ~1.5 kcal mol^{-1} (data not shown). The r_1 and r_2 reaction coordinates yield barriers similar in shape and in barrier height (barrier = ~1.0 kcal mol^{-1}). These results provide a further indication that addition of glutathione to CDNB has a low barrier in the enzyme.

Product release is believed to be rate-limiting in the turnover of CDNB with GST M1-1 (*9*, *16*). The low barrier calculated for the chemical step here is consistent with this proposal. Apparent activation energies of 1.8 kcal mol^{-1} and 3.4 kcal mol^{-1} for the reaction with CDNB for two GST isoenzymes were recently reported for *Bulinus truncatus* (*46*). These isoenzymes have not yet been classified, but the results were stated to be consistent with those of mammalian GSTs (*46*). It is thought that product release is not rate-limiting in these *Bulinus truncatus* isoenzymes, and thus the activation energies quoted may be a good indication of the barrier of the chemical reaction. Therefore our calculated barrier for the chemical step of ~1.0 kcal mol^{-1} overall appears to be reasonable.

Free Energy Calculations and Comparison with Experiment for the Reaction in Solution. The simulations of the nonenzymic reaction in water gave a free energy barrier of ~9.5 kcal mol^{-1} (Figure 2) for the nucleophilic attack of the glutathione anion on CDNB. This is significantly larger than the corresponding barrier in the enzyme. The simulations clearly show an important catalytic effect of the enzyme in lowering the barrier to this reaction.

Experiments indicate an apparent free energy barrier of 23.8 kcal mol^{-1} for reaction of the GS^- anion with CDNB in solution (at pH 8.0, at a CDNB concentration of 0.01 mM and a saturating, 2 mM (*47*) GSH concentration) (*48*). However, the experimental data was reported as effective first-order rate constants. To obtain results for standard states (i.e., the standard activation free energy, 1 M concentration for both reactants), the experimental effective first-order rates are corrected here for concentrations. This allows comparison to the calculated barrier, when this is also corrected for concentration as described below. Correcting the experimental findings for changing the concentration of CDNB and GSH to 1 M lowers the experimental barrier by 6.8 kcal mol^{-1} and 3.7 kcal mol^{-1}, respectively, giving a standard activation free energy barrier of 13.3 kcal mol^{-1}. This experimental barrier also contains a contribution due to the dissociation of the GSH thiol at pH 8 (the experiments were performed at pH 8). The pK_a of the thiol is approximately 9, so the free energy cost of dissociation at pH 8 is 1.4 kcal mol^{-1}. The experimental (standard state) barrier for the reaction of the thiolate with CDNB is therefore (13.3−1.4 =) 11.9 kcal mol^{-1}.

As Warshel has discussed (*23*), simulation results for reaction in solution should also be corrected appropriately for concentration effects to obtain the standard activation free energy. These corrections are to account for bringing together the two reactants in the same solvent shell, and bringing them into the correct orientation for reaction, the so-called "cratic" free energy (*49*). For a bimolecular reaction Warshel and co-workers have estimated this free energy correction for bringing together two reactants (in 1 M concentration) to be 2.4 kcal mol^{-1} (*50*): the value corresponds well to the 55 M correction which was popular previously (*51*). With this correction, the calculated (standard state) barrier is (9.5 + 2.4 =) 11.9 kcal mol^{-1}, in excellent agreement with standard free energy barrier from experiment.

The C_1-Cl and C_1-S bond lengths are similar in the Meisenheimer complex, so it is located around $r_1 = 0.0$ Å on the reaction pathway. When a snapshot structure from this region was subject to unrestrained energy minimization, it was found to have a geometry very similar to that found for the Meisenheimer complex from the reaction in the enzyme. There is a shoulder on the free energy profile at $r_1 = 0.05$ Å but no barrier, indicating that in solution the Meisenheimer complex is not stable, and would not be expected to have a measurable lifetime. However, the stability observed in the unrestrained energy optimization indicates that the Meisenheimer complex corresponds to a

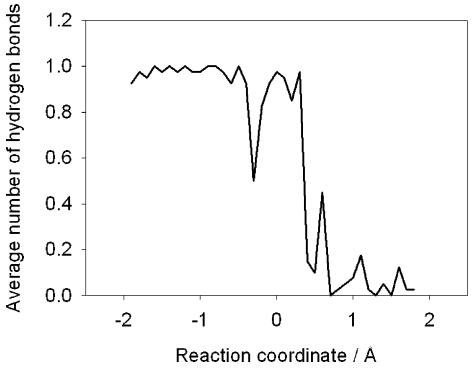

FIGURE 3: Hydrogen bonding between phenolic hydroxyl group of Tyr6 and sulfhydryl group of glutathione along the reaction coordinate, for reaction of CDNB in the wild-type M1-1 GST enzyme.

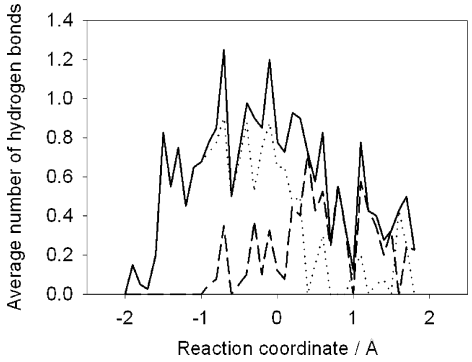

FIGURE 4: A conserved water molecule in the active site of the wild-type M1-1 GST enzyme forms hydrogen bonds to the *p*-nitro group oxygens of CDNB. The dotted line represents the average number of hydrogen bonds between the conserved water molecule and O41 of CDNB, the dashed line between the water and O42 of CDNB, and the solid line represents the sum of these two values for the reaction in the wild-type enzyme.

shallow minimum on the potential energy surface. The free energy change for chloride dissociation from the Meisenheimer complex is -22.3 kcal mol^{-1}, showing that the reaction is highly favorable (Figure 2).

Previous *ab initio* quantum chemical calculations on small models with a continuum solvation model indicated a stable intermediate in aqueous solution, but with only a small barrier to dissociation (1.6 kcal mol^{-1}) (*25*). However, these calculations were performed using a dielectric continuum solvent model and gas-phase geometries. Here we employ an explicit, detailed solvent model and specifically parameterized QM model. Continuum solvent models have known limitations, particularly for modeling reactions. An explicit description of solvation is preferable, although clearly as with any modeling method, the QM/MM approach also involves important approximations. Both our calculations, and the previous findings of Zheng and Ornstein (*25*), indicate that at best the Meisenheimer complex is expected to be only marginally stable in solution.

Hydrogen Bonding in the Wild-Type M1-1 GST Reaction. GSTs exhibit broad substrate specificity and detoxify many different compounds, so different, specific mechanisms to bind each compound tightly are unlikely (*25*). Instead, GST active sites are able to accommodate a wide variety of substrates, and catalyze their conjugation with GSH. It is believed that GSTs catalyze nucleophilic attack by deprotonating GSH to GS$^-$ and desolvating and crucially stabilizing the glutathione thiolate anion (*52*). Of course, for different substrates and different GSTs, the rate may be limited by different steps in the overall cycle (e.g., the chemical step, or product release).

A conserved active site tyrosine residue at the GSH binding site of certain GSTs (Tyr8 for α, Tyr6 or Tyr7 for μ, Tyr7 for π classes of GST, respectively) has been implicated in catalysis (*1*, *8*, *28*, *53*−*56*). The phenolic hydroxyl group of this tyrosine residue stabilizes the deprotonated thiolate anion by hydrogen bonding to the sulfhydryl group of GSH. Initially there is an average of 0.94 hydrogen bond between the hydroxyl group of Tyr6 and the thiolate in the active site. After the Meisenheimer complex is formed ($r_1 > 0.0$ Å) the thiolate is no longer present and this interaction is lost; the number of hydrogen bonds between the hydroxyl group of Tyr6 and the sulfur rapidly decreases to an average of 0.09 (Figure 3). This reduction in hydrogen bonding along the reaction coordinate is in accord with crystallographic studies: in the transition state analogue crystal structure (4GST) the distance between the phenolic hydroxyl group of Tyr6 and the sulfhydryl group of glutathione is 3.2 Å, while the distance between the same two atoms in the product complex (5GST) is 3.6 Å (*28*). The results here for the CDNB reaction are in contrast to our findings for the GST reaction with phenanthrene 9,10-oxide, where the hydrogen bond between the thiolate sulfur and Tyr6 is present throughout all simulations (*14*). Following conjugation of the glutathione to CDNB, the product moves slightly out of the active site away from Tyr6; this conformational change is more limited in the phenanthrene 9,10-oxide simulations. It should be noted that in the previous work the Tyr6 side chain was modeled as QM while in the present study it is modeled MM.

It has been proposed that Tyr6 alone does not effectively stabilize the glutathione thiolate and that the presence of the Arg107 (for μ class GSTs) side chain near the active site pocket is also required (*57*). Both thermodynamic and kinetic data indicate that Arg107 is specifically involved in enhancing the binding affinity for GS$^-$ thiolate anion relative to that of the protonated GSH form (*57*). Although we find that there are no hydrogen bonds between Arg107 and the substrate, the mean distance of 4.6 Å ± 0.3 Å to the *p*-nitro group of CDNB in the intermediate implies that an electrostatic stabilization rather than hydrogen bond formation is present.

A crystallographically observed water molecule (of which the oxygen atom is referred to as O1 (*28*)) forms hydrogen bonds with the *p*-nitro group oxygens of CDNB (O41 and O42) throughout the reaction (Figure 4). The hydrogen bonding is largely through one hydrogen atom (H1) of the water molecule. The extent of hydrogen bonding is greatest between -1.0 Å $< r_1 <$ 0.5 Å, where this atom is involved in hydrogen bonding to both oxygens of the *p*-nitro group. This conserved water molecule is held in place throughout the reaction by hydrogen bonds between this water's oxygen and Arg107 (average number of hydrogen bonds ± standard deviation, 0.99 ± 0.02) and between the H2 atom of the water and Gln165 (0.97 ± 0.3).

For the reaction in the enzyme complex, we find the hydrogen bonding between the solvent and the reacting Cl and S atoms is at a minimum in the Meisenheimer complex

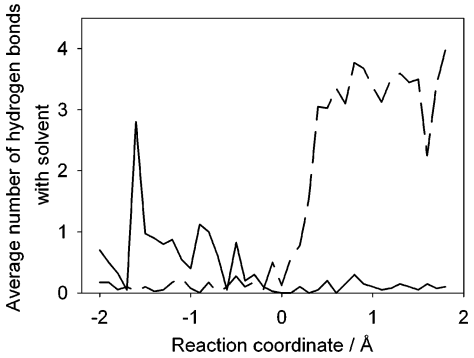

FIGURE 5: The solid line shows the average number of hydrogen bonds donated to the sulfur atom of glutathione by water molecules during the reaction in the wild-type M1-1 GST enzyme. The dashed line shows the average number of hydrogen bonds between the chloride/chlorine of CDNB and the solvent.

(at $r_1 = \sim 0.0$ Å) (Figure 5). During the reaction, the thiolate sulfur becomes less well solvated, as shown by the decrease in hydrogen bonding from the solvent to approximately none after $r_1 = \sim 0.0$ Å. The chloride is shown to be increasingly solvated after $r_1 = \sim 0.0$ Å: see the increase of hydrogen bonds after this point as shown in Figure 5. This is to be expected as the chloride ion dissociates.

In our previous work on the conjugation of glutathione to phenanthrene 9,10-oxide catalyzed by M1-1 GST, the average number of hydrogen bonds from the solvent and protein to sulfur was shown to decrease from ~3.5 to 1.5 as the reaction proceeded. It was also shown that the number of hydrogen bonds to the oxygen (O5) of phenanthrene 9,10-oxide changes from ~1.5 to more than 3. Hydrogen bonding to the protein was approximately constant throughout the reaction. These results showed desolvation of the thiolate sulfur and an increase in solvation of the oxygen (O5) as the reaction proceeds (*14*). Similarly here, the thiolate sulfur of GST is well solvated initially, accepting many (up to 3) hydrogen bonds from water in the reactant complex. The number of hydrogen bonds from water to the sulfur decreases markedly during the reaction, while the number of hydrogen bonds to chlorine/chloride increases significantly (to between 3 and 4 on average) as it dissociates (Figure 5).

Mulliken Charge Analysis of the Wild-Type M1-1 GST Reaction. Mulliken atomic charges often do not provide a good description of electronic distributions in molecules. However, Mulliken charge analysis can provide a useful analysis of *changes* in electronic populations along the reaction path (*58*). In a QM/MM system, such as that described above, Mulliken charges include the effect of polarization by the protein and solvent water molecules. AM1-SRP/CHARMM QM/MM Mulliken atomic charges were calculated for structures along the reaction pathway using CHARMM. Each structure was the final "snapshot" structure following 30 ps of simulation. Structural fluctuations will give rise to changes in charge, but analysis of just these structures should show important trends during the reaction. All atomic charges are given in atomic units (units of *e*).

There is very little change in the atomic charges for the *o*- and *p*-nitro groups of CDNB, for the hydrogens on the ring of CDNB, or for the CH_2 QM part of GSH. As expected, chloride leaves with a charge of approximately −1, while the charge on the sulfur becomes less negative; at the

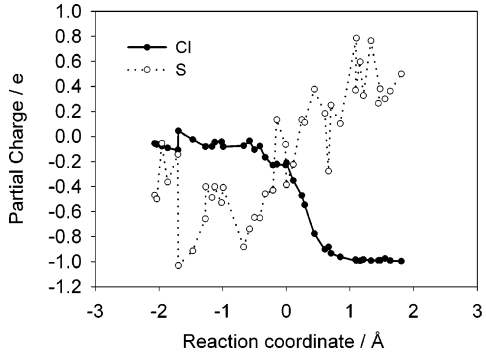

FIGURE 6: AM1-SRP/CHARMM22 QM/MM Mulliken charges along the reaction coordinate in the wild-type enzyme complex. The solid line represents the Mulliken charges for chlorine/chloride (Cl, which is released from CDNB during the reaction), and the dotted line represents the Mulliken charges for the sulfur of glutathione.

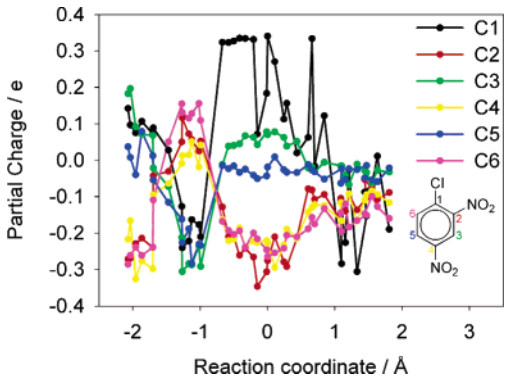

FIGURE 7: AM1-SRP/CHARMM22 QM/MM Mulliken charges of ring carbons along the reaction path, for the reaction of CDNB in the wild-type M1-1 GST enzyme.

Meisenheimer complex ($r_1 = 0.0$ Å) the charges of the two atoms are approximately equal (~−0.3) (Figure 6). In CDNB, C_1, C_3, and C_5 have a more positive charge than C_2, C_4, and C_6 (Figure 7). At $r_1 = \sim -1.0$ Å, where the barrier to formation of the Meisenheimer complex lies, there is a change in the Mulliken charges: C_2, C_4, and C_6 take a more positive charge than at more negative values of r_1 and C_1, C_3, and C_5 take a more negative charge. From the barrier at $r_1 = \sim -1.0$ Å C_2, C_4, and C_6 decrease in partial charge whereas C_5, C_3, and especially C_1 increase in charge to a maximum at the Meisenheimer complex. After the chloride has left the Meisenheimer complex, all the ring carbon charges converge and there is an equal spread of charge around the ring.

Tyr6Phe. The hydroxyl group of Tyr6 is important for lowering the pK_a of the bound GSH thiol (*8*, *11*). In the calculated free energy profile for the Tyr6Phe mutant enzyme there is a larger barrier to form the Meisenheimer complex of ~3.8 kcal mol^{-1} than in the wild-type enzyme. The energy change for Meisenheimer complex formation is ~−14.4 kcal mol^{-1}. There is a minimum at $r_1 = 0.0$ Å indicating that the Meisenheimer complex is present as an intermediate. Unrestrained QM/MM energy minimization of a snapshot from this region yielded a geometry very similar to the Meisenheimer complex found from the reaction in the wild-type enzyme, indicating that this corresponds to a (potential) energy minimum. Again, similar to the reaction in the wild-type enzyme, there is only a ~0.8 kcal mol^{-1} barrier to dissociation of chloride in the mutant enzyme, implying that

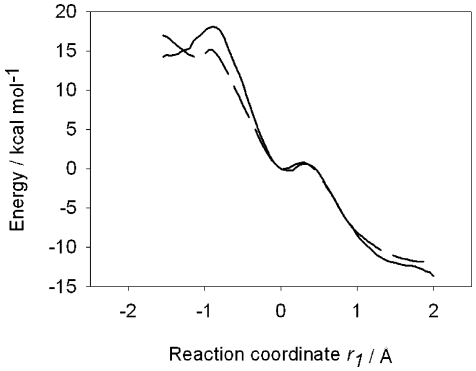

FIGURE 8: Calculated AM1-SRP/CHARMM22 free energy profile for the reaction of glutathione anion with CDNB in the Tyr6Phe mutant M1-1 GST (solid line). For comparison, the free energy profile of the reaction in the wild-type enzyme is included (dashed line). The curves are aligned taking the Meisenheimer complex as the zero of free energy in each case.

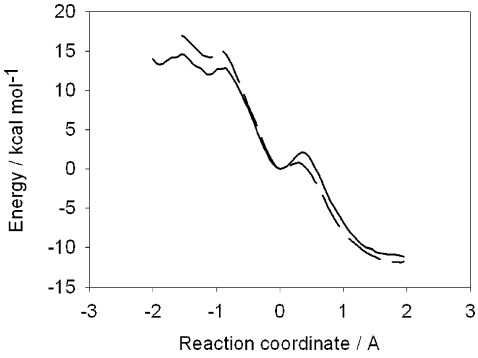

FIGURE 9: Free energy profile for the reaction of glutathione anion with CDNB in the Tyr115Phe mutant M1-1 GST (solid line). For comparison the free energy profile of the reaction in the wild-type enzyme is included (dashed line). The curves are aligned taking the Meisenheimer complex as the zero of free energy in each case.

the Meisenheimer intermediate is very unstable, and would be expected to have a negligible lifetime. The free energy change for dissociation of the chloride is ~ -13.0 kcal mol^{-1} (Figure 8).

There is a possibility that the GS−CDNB complex in the Tyr6Phe mutant GST is actually a low-populated, highly reactive state. GST needs to form GS$^-$ for efficient reaction, and this requires the thiolate to be stabilized. In the Tyr6Phe mutant the thiolate is not as well stabilized as in the wild-type enzyme, due to the loss of the hydrogen bond between the phenolic hydroxyl group of Tyr6 and the sulfhydryl group of GS$^-$. However, the Tyr6Phe mutant still possesses catalytic activity in comparison to the reaction in solution (*8*). It has been proposed that in the Tyr6Phe mutant an active site water hydrogen bonds to the thiolate (*54*). This hydrogen bond along with the electrostatic interaction of Arg107 (*57*) is believed to stabilize GS$^-$ in the Tyr6Phe mutant GST. In fact, we observe GS$^-$ stabilizing hydrogen bonds between the thiolate and up to four water molecules in the Tyr6Phe mutant before the formation of the Meisenheimer complex.

The energy profile of the reaction pathway found here is similar to the wild-type enzyme after the Meisenheimer complex has been formed: this can be understood as Tyr6 does not play a part in stabilizing the GS−CDNB complex (see Figure 3). This implies that Tyr6 is not essential in catalyzing the attack of the thiolate on CDNB, but it does have a significant role in catalysis by lowering the pK_a of the thiol of bound GSH.

Tyr115Phe. Tyr115 is thought to participate in both the chemical and physical aspects of the GST mechanism (*9*). The calculated free energy profile for the Tyr115Phe mutant is similar to that for the wild-type enzyme (Figure 9). Similarly to the wild-type enzyme, there is a small barrier of $\sim$1 kcal mol^{-1} at $r_1 = -1.0$ Å to form the Meisenheimer complex from the glutathione anion and CDNB. The energy change for complex formation from the reactant complex is ~ -12.0 kcal mol^{-1}. A minimum is present at $r_1 = 0.0$ Å, and minimization of a snapshot from this region yielded a geometry that was very similar to the Meisenheimer complex in the wild-type enzyme. There is approximately a 2 kcal mol^{-1} barrier for the dissociation of the chloride anion from this Meisenheimer intermediate. This indicates that the Meisenheimer complex is a slightly more stable intermediate in the Tyr115Phe mutant enzyme complex than in the wild-type. The energy change for chloride dissociation is ~ -11.0 kcal mol^{-1}.

Although the energy changes in the mutant enzyme are smaller and the barrier for dissociation of the chloride from the Meisenheimer intermediate is slightly larger than the wild-type enzyme, the free energy profiles of the wild-type and the Tyr115Phe mutant are similar. There is no significant chemical change due to the Tyr115Phe mutation. Therefore, the increase in catalytic efficiency seen experimentally for the Tyr115Phe mutant enzyme should not be attributed to a significant effect on the reaction pathway leading to Meisenheimer formation followed by chloride release. Based on literature data, the effect is likely to be due to a difference in the rate of product release (*9*). This is in contrast to the effect seen in the equivalent reaction with phenanthrene 9,10-oxide, for which experiments show that replacement of Tyr115 with phenylalanine results in a 100-fold decrease in catalytic power with the phenanthrene 9,10-oxide substrate. It is thought that the Tyr115 side chain acts as a hydrogen bond donor to the oxirane oxygen of phenanthrene 9,10-oxide stabilizing the transition states for opening of the ring (*9*, *14*). The fact that our results for both substrates concur with experiment for this mutation lends confidence to the accuracy of our approach.

Met108Ala. Met108 is thought to make a significant contribution to the binding of CDNB (*10*). The calculated free energy profile for the Met108Ala mutant is also similar to that for the wild-type enzyme (Figure 10). Again, there is a small barrier at $r_1 = -1.0$ Å to form the Meisenheimer complex from the glutathione anion and CDNB of $\sim$0.8 kcal mol^{-1}, however this barrier is broader than found with the wild-type enzyme. The Meisenheimer complex lies $\sim$11.0 kcal mol^{-1} lower in free energy than the reactant complex. A minimum is present at $r_1 = 0.0$ Å, and there is approximately a 1 kcal mol^{-1} barrier dissociation of chloride from this intermediate. The energy change for dissociation of the chloride from the Meisenheimer complex is ~ -12.9 kcal mol^{-1}. This indicates that, as in the wild-type enzyme, the Meisenheimer complex is present as a rather unstable intermediate in the Met108Ala mutant. The similarity between the two free energy profiles is as expected as Met108 appears not to be involved in the chemical reaction. Instead this residue appears to be involved in the binding of CDNB, and may affect the rate of product release (*10*).

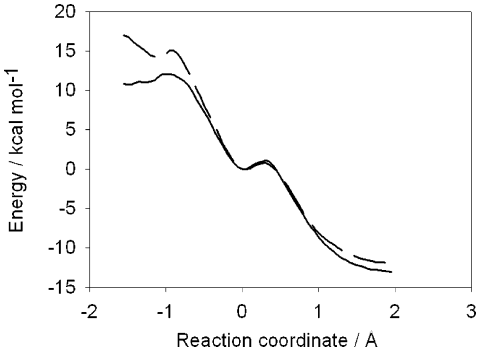

FIGURE 10: Free energy profile for the reaction of glutathione anion with CDNB in the Met108Ala mutant M1-1 GST (solid line). For comparison, the free energy profile of the reaction in the wild-type enzyme is included (dashed line). The curves are aligned taking the Meisenheimer complex as the zero of free energy.

CONCLUSIONS

QM/MM simulations with a specifically parameterized AM1-SRP method give results in excellent agreement with experiment for the reaction of glutathione anion with CDNB, in M1-1 GST and in solution. The simulations indicate that the Meisenheimer complex is an intermediate in the enzyme, but there is only a very small barrier ($\sim$1 kcal mol^{-1}) to dissociation of chloride from this intermediate. There is a small barrier (1 kcal mol^{-1}) to form the Meisenheimer intermediate from the glutathione anion and CDNB in the enzyme. In the nonenzymatic reaction in solution there is a larger barrier of 9.5 kcal mol^{-1} to formation of the Meisenheimer complex, and this complex is found to be unstable in solution. GST M1-1 lowers the energy barrier for formation of the Meisenheimer complex by $\sim$8.5 kcal mol^{-1} compared to the reaction in solution.

The effects of some key single point mutations on the chemical step have also been analyzed. The possible changes that mutagenesis can cause in protein structure (*59*) or chemical mechanism (*60*) can complicate the interpretation of experimental results. The ability to model the reaction accurately allows mutation studies to be performed computationally to interpret experimental results and analyze mechanisms in atomic detail. Simulations are playing an increasingly important role in the analysis of the mechanisms and specificity of xenobiotic (e.g., drug) metabolism (*20*, *61*, *62*). Modeling the effects of the Tyr6Phe mutation emphasizes the important role of Tyr6 in GST for lowering the pK_a of the thiol of bound GSH. Results from simulations of the Tyr115Phe and Met108Ala mutant GSTs are similar to those for the wild-type enzyme, indicating that Tyr115 and Met108 are not involved in the chemical reaction. Experimental work shows a slight increase in catalytic activity for the Tyr115Phe mutant (*9*) and for Met108Ala (*10*). The effect of these two mutations is found to be small, confirming that the mutations do not exert their effect by changing the chemical reaction in the active site of GST. The results here are consistent with the suggestion that mutating Tyr115 or Met108 affects the rate of product release.

SUPPORTING INFORMATION AVAILABLE

AM1-SRP parameters for modeling the reaction of glutathione S-transferase with 1-chloro-2,4-dinitrobenzene. This material is available free of charge via the Internet at http://pubs.acs.org.

REFERENCES

1. Armstrong, R. N. (1997) Structure, catalytic mechanism and evolution of the glutathione transferases, *Chem. Res. Toxicol. 10*, 2−18.
2. International Human Genome Sequencing Consortium (2004) *Nature 431*, 931−945.
3. Rushmore, T. H., and Pickett, C. B. (1993) Glutathione S-transferases, structure, regulation, and therapeutic implication, *J. Biol. Chem. 268*, 11475−11478.
4. Eaton, D. L., and Bammler, T. K. (1999) Concise review of the glutathione S-transferases and their significance to toxicology, *Toxicol. Sci. 49*, 156−164.
5. del Carmen Terrones Saldívar, M., Juárez, F. J., Viramontes, J. L., Rodríguez Vázquez, M. L., and Posadas del Río, F. A. (2004) Glutathione S-transferases and esterases in placenta after normal and pre-eclamptic pregnancies, *Placenta 25*, 311−336.
6. Hansson, L. O., Bolton-Grob, R., Massoud, T., and Mannervik, B. (1999) Evolution of differential substrate specificities in mu class glutathione transferases probed by DNA shuffling, *J. Mol. Biol. 287*, 265−276.
7. Ivarsson, Y., Mackey, A. J., Edalat, M., Pearson, W. R., and Mannervik, B. (2003) Identification of residues in glutathione transferase capable of driving functional diversification in evolution, *J. Biol. Chem. 278*, 8733−8738.
8. Liu, S., Zhang, P., Ji, X., Johnson, W. W., Gilliland, G. L., and Armstrong, R. N. (1992) Contribution of tyrosine 6 to the catalytic mechanism of isoenzyme 3-3 of glutathione S-transferase, *J. Biol. Chem. 267*, 4296−4299.
9. Johnson, W. W., Liu, S., Ji, X., Gilliland, G. L., and Armstrong, R. N. (1993) Tyrosine 115 participates both in chemical and physical steps of the catalytic mechanism of a glutathione S-transferase, *J. Biol. Chem. 268*, 11508−11511.
10. McCallum, S. A., Hitchens, T. K., Torborg, C., and Rule, G. S. (2000) Ligand-induced changes in the structure and dynamics of a human class mu glutathione S-transferase, *Biochemistry 39*, 7343−7356.
11. Xiao, G. Y., Liu, S. X., Ji, X. H., Johnson, W. W., Chen, J. H., Parsons, J. F., Stevens, W. J., Gilliland, G. L., and Armstrong, R. N. (1996) First-sphere and second-sphere electrostatic effects in the active site of a class Mu glutathione transferase, *Biochemistry 35*, 4753−4765.
12. Katusz, R. M., and Colman, R. F. (1991) S-(4-Bromo-2,3-dioxobutyl)glutathione: a new affinity label for the 4−4 isoenzyme of rat liver glutathione S-transferase, *Biochemistry 30*, 11230−11238.
13. Ji, X., Zhang, P., Armstrong, R. N., and Gilliland, G. L. (1992) The three-dimensional structure of a glutathione S-transferase from the mu gene class. Structural analysis of the binary complex of isoenzyme 3-3 and glutathione at 2.2 Å resolution, *Biochemistry 31*, 10169−10184.
14. Ridder, L., Rietjens, I. M. C. M., Vervoort, J., and Mulholland, A. J. (2002) QM/MM free energy simulation of the glutathione S-transferase (M1-1) reaction with phenanthrene 9,10-oxide, *J. Am. Chem. Soc. 124*, 9926−9936.
15. Ji, X. H., Johnson, W. W., Sesay, M. A., Dickert, L., Prasad, S. M., Ammon, H. L., Armstrong, R. N., and Gilliland, G. L. (1994) Structure and function of the xenobiotic substrate-binding site of a glutathione-S-transferase as revealed by X-ray crystallographic analysis of product complexes with the diastereomers of 9-(S-glutathionyl)-10-hydroxy-9,10-dihydrophenanthrene, *Biochemistry 33*, 1043−1052.
16. Zhang, P., Liu, S., Shan, S. O., Ji, X., Gilliland, G. L., and Armstrong, R. N. (1992) Modular mutagenesis of exons 1, 2, and 8 of a glutathione S-transferase from the Mu class. Mechanistic and structural consequences for chimeras of isoenzyme 3-3, *Biochemistry 31*, 10185-10193.
17. Rietjens, I. M. C. M., Soffers, A. E. M. F., Hooiveld, G., Veeger, C., and Vervoort, J. (1995) Quantitative structure-activity relationships based on computer calculated parameters for the overall rate of glutathione S-transferase catalyzed conjugation of a series of fluoronitrobenzenes, *Chem. Res. Toxicol. 8*, 481−488.
18. Soffers, A. E. M. F., Ploemen, J. H. T. M., Moonen, M. J. H., Wobbes, T., van Ommen, B., Vervoort, J., van Bladeren, P. J.,

and Rietjens, I. M. C. M. (1996) Regioselectivity and quantitative structure-activity relationships for the conjugation of a series of fluoronitrobenzenes by purified glutathione S-transferase enzymes from rat and man, *Chem. Res. Toxicol. 9*, 638−646.
19. Warshel, A., and Levitt, M. (1976) Theoretical studies of enzymic reactions: dielectric, electrostatic and steric stabilization of the carbonium ion in the reaction of lysozyme, *J. Mol. Biol. 103*, 227−249.
20. Mulholland, A. J. (2005) Modelling enzyme reaction mechanisms, specificity and catalysis, *Drug Discovery Today 10*, 1393−1402.
21. Rossi, I., and Truhlar, D. G. (1995) Parameterization of NDDO wavefunctions using genetic algorithms. An evolutionary approach to parameterizing potential energy surfaces and direct dynamics calculations for organic reactions, *Chem. Phys. Lett. 233*, 231−236.
22. Masgrau, L., Roujeinikova, A., Johannissen, L. O., Hothi, P., Basran, J., Ranaghan, K. E., Mulholland, A. J., Sutcliffe, M. J., Scrutton, N. S., and Leys, D. (2006) Atomic description of an enzyme reaction dominated by proton tunneling, *Science 312*, 237−241.
23. Warshel, A. (1997) *Computer modeling of Chemical Reactions in Enzymes and Solutions*, John Wiley & Sons, New York.
24. Bentzien, J., Muller, R. P., Florian, J., and Warshel, A. (1998) Hybrid ab Initio quantum mechanics/molecular mechanics calculations of free energy surfaces for enzymatic reactions: The nucleophilic attack in subtilisin, *J. Phys. Chem. B. 102*, 2293−2301.
25. Zheng, Y., and Ornstein, R. L. (1997) Mechanism of nucleophilic aromatic substitution of 1-chloro-2,4-dinitrobenzene by glutathione in the gas phase and in solution. Implications for the mode of action of glutathione S-transferases, *J. Am. Chem. Soc. 119*, 648−655.
26. Xu, D., Guo, H., Gao, J., and Cui, Q. (2004) A QM/MM study of a nucleophilic aromatic substitution reaction catalyzed by 4-chlorobenzoyl-CoA dehalogenase, *Chem. Commun.* 892−893.
27. Graminski, G. F., Zhang, P., Sesay, M. A., Ammon, H. L., and Armstrong, R. N. (1989) Formation of the 1-(S-glutathionyl)-2,4,6-trinitrocyclohexadienate anion at the active site of glutathione S-transferase: evidence for enzymic stabilization of σ-complex intermediates in nucleophilic aromatic substitution reactions, *Biochemistry 28*, 6252−6258.
28. Ji, X., Armstrong, R. N., and Gilliland, G. L. (1993) Snapshots along the reaction coordinate of an S_NAr reaction catalyzed by glutathione transferase, *Biochemistry 32*, 12949−12954.
29. Liu, H. Y., Muller-Plathe, F., and van Gunsteren, W. F. (1996) A combined quantum/classical molecular dynamics study of the catalytic mechanism of HIV protease, *J. Mol. Biol. 261*, 454−469.
30. Thomas, A., Jourand, D., Bret, C., Amara, P., and Field, M. J. (1999) Is there a covalent intermediate in the viral neuraminidase reaction? A hybrid potential free-energy study, *J. Am. Chem. Soc. 121*, 9693−9702.
31. Proust-De Martin, F., Dumas, R., and Field, M. J. (2000) A hybrid-potential free-energy study of the isomerization step of the acetohydroxy acid isomeroreductase reaction, *J. Am. Chem. Soc. 122*, 7688−7697.
32. Brooks, C. L., III, and Karplus, M. (1989) Solvent effects on protein motion and protein effects on solvent motion-dynamics of the active site region of lysozyme, *J. Mol. Biol. 208*, 159−181.
33. MacKerell, A. D., Bashford, D., Bellott, R. L., Dunbrack, R. L., Evanseck, J. D., Field, M. J., Fischer, S., Gao, J., Guo, H., Ha, S., Joseph-McCarthy, D., Kuchnir, L., Kuczera, K., Lau, F. T. K., Mattos, C., Michnick, S., Ngo, T., Nguyen, D. T., Prodhom, B., Reiher, W. E., Roux, B., Schlenkrich, M., Smith, J. C., Stote, R., Straub, J., Watanabe, M., Wiorkiewicz-Kuczera, J., Yin, D., and Karplus, M. (1998) All-atom empirical potential for molecular modeling and dynamics studies of proteins, *J. Phys. Chem. B 102*, 3586−3616.
34. Reuter, N., Dejaegere, A., Maigret, B., and Karplus, M. (2000) Frontier bonds in QM/MM methods: A comparison of different approaches, *J. Phys. Chem. A 104*, 1720−1735.
35. MacKerell, A. D., Wiorkiewicz-Kuczera, J., and Karplus, M. (1995) An all-atom empirical energy function for the simulation of nucleic acids, *J. Am. Chem. Soc. 117*, 11946−11975.
36. Mulholland, A. J., and Richards, W. G. (1997) Acetyl-CoA enolization in citrate synthase: A quantum mechanical molecular mechanical (QM/MM) study, *Proteins 27*, 9−25.
37. Brooks, B. R., Bruccoleri, R. E., Olafson, B. D., States, D. J., Swaminathan, S., and Karplus, M. (1983) CHARMM−a program for macromolecular energy, minimization and dynamics calculations, *J. Comput. Chem. 4*, 187−217.
38. Torrie, G. M., and Valleau, J. P. (1974) Monte Carlo free energy estimates using non-Boltzmann sampling: Application to the subcritical Lennard-Jones fluid, *Chem. Phys. Lett. 28*, 578−581.
39. Bartels, C., and Karplus, M. (1997) Multidimensional adaptive umbrella sampling: Applications to main chain and side chain peptide conformations, *J. Comput. Chem. 18*, 1450−1462.
40. Kumar, S., Bouzida, D., Swendsen, R. H., Kollman, P. A., and Rosenberg, J. M. (1992) Multidimensional free-energy calculations using the weighted histogram analysis method, *J. Comput. Chem. 13*, 1011−1021.
41. Hadfield, A. T., and Mulholland, A. J. (1999) Active-site dynamics of ASADH-a bacterial biosynthetic enzyme, *Int. J. Quantum Chem. 73*, 137−146.
42. Dewar, M. J. S., Zoebisch, E. G., Healy, E. F., and Stewart, J. J. P. (1985) AM1: a new general purpose quantum mechanical molecular model, *J. Am. Chem. Soc. 107*, 3902−3909.
43. Bash, P. A., Ho, L. L., MacKerell, A. D., Levine, D., and Hallstrom, P. (1996) Progress toward chemical accuracy in the computer simulation of condensed phase reactions, *Proc. Natl. Acad. Sci. U. S. A. 93*, 3698−3703.
44. Proceedings of the 1993 ACM/SIGAPP symposium on applied computing, Indianapolis, IN (1993).
45. Mulholland, A. J., Grant, G. H., and Richards, W. G. (1993) Computer modelling of enzyme catalysed reaction mechanisms, *Protein Eng. 6*, 133−147.
46. Abdalla, A. M., El-Mogy, M., Farid, N. M., and El-Sharabasy, M. (2006) Two glutathione S-transferase isoenzymes purified from Bulinus truncatus (Gastropoda: Planorbidae), *Comp. Biochem. Physiol., Part B: Biochem. Mol. Biol. 143*, 76−84.
47. Pal, A., Seidel, A., Xia, H., Hu, X., Srivastava, S. K., Oesch, F., and Singh, S. V. (1999) Specificity of murine glutathione S-transferase isozymes in the glutathione conjugation of (−)-*anti*- and (+)-*syn*-stereoisomers of benzo[*g*]chrysene 11,12-diol 13,14-epoxide, *Carcinogenesis 20*, 1997−2001.
48. Huskey, S. W., Huskey, W. P., and Lu, A. Y. H. (1991) Contributions of thiolate "desolvation" to catalysis by glutathione S-transferase isozymes 1-1 and 2-2: evidence from kinetic solvent isotope effects, *J. Am. Chem. Soc. 113*, 2283−2290.
49. Roca, M., Marti, S., Andres, J., Moliner, V., Tunon, I., Bertran, J., and Williams, I. H. (2003) Theoretical modeling of enzyme catalytic power: Analysis of "cratic" and electrostatic factors in catechol O-methyltransferase, *J. Am. Chem. Soc. 125*, 7726−7737.
50. Villá, J., Štrajbl, M., Glennon, T. M., Sham, Y. Y., Chu, Z. T., and Warshel, A. (2000) How important are entropic contributions to enzyme catalysis?, *Proc. Natl. Acad. Sci. U.S.A. 97*, 11899−11904.
51. Štrajbl, M., Florián, J., and Warshel, A. (2000) Ab initio evaluation of the potential surface for general base-catalyzed methanolysis of formamide: A reference solution reaction for studies of serine proteases, *J. Am. Chem. Soc. 122*, 5354−5366.
52. Armstrong, R. N. (1991) Glutathione S-transferases: reaction mechanism, structure, and function, *Chem. Res. Toxicol. 4*, 131−140.
53. Dietze, E. C., Ibarra, C., Dabrowski, M. J., Bird, A., and Atkins, W. M. (1996) Rational modulation of the catalytic activity of A1-1 glutathione S-transferase: Evidence for incorporation of an on-face (π···HO-Ar) hydrogen bond at tyrosine-9, *Biochemistry 35*, 11938−11944.
54. Zheng, Y. J., and Ornstein, R. L. (1997) Role of active site tyrosine in glutathione S-transferase: Insights from a theoretical study on model systems, *J. Am. Chem. Soc. 119*, 1523−1528.
55. Xiao, G., Parsons, J. F., Tesh, K., Armstrong, R. N., and Gilliland, G. L. (1998) Conformational changes in the crystal structure of rat glutathione transferase M1-1 with global substitution of 3-fluorotyrosine for tyrosine, *J. Mol. Biol. 281*, 323−339.
56. Rignanese, G. M., De Angelis, F., Melchionna, S., and De Vita, A. (2000) Glutathione transferase: A first-principles study of the active site, *J. Am. Chem. Soc. 122*, 11963−11970.
57. Patskovsky, Y. V., Patskovska, L. N., and Listowsky, I. (2000) The enhanced affinity for thiolate anion and activation of enzyme-bound glutathione is governed by an arginine residue of human Mu class glutathione S-transferases, *J. Biol. Chem. 275*, 3296−3304.

58. Jensen, F. (1999) *Introduction to Computational Chemistry*, John Wiley & Sons, Chichester, U.K.
59. Karplus, M., Evanseck, J. D., Joseph, D., Bash, P. A., and Field, M. J. (1992) Simulation analysis of triose phosphate isomerase-conformational transition and catalysis, *Faraday Discuss. 93*, 239−248.
60. Nickbarg, E. B., Davenport, R. C., Petsko, G. A., and Knowles, J. R. (1988) Triosephosphate isomerase-removal of a putatively electrophilic histidine residue results in a subtle change in catalytic mechanism, *Biochemistry 27*, 5948−5960.
61. Bathelt, C. M., Zurek, J., Mulholland, A. J., and Harvey, J. N. (2005) Electronic structure of compound I in human isoforms of cytochrome P450 from QM/MM modeling, *J. Am. Chem. Soc. 127*, 12900−12908.
62. Bathelt, C. M., Ridder, L., Mulholland, A. J., and Harvey, J. N. (2004) Mechanism and structure-reactivity relationships for aromatic hydroxylation by cytochrome P450, *Org. Biomol. Chem. 2*, 2998−3005.

BI0622827